Chemical Engineering Science xxx (xxxx) xxx

Contents lists available at ScienceDirect

Chemical Engineering Science

journal homepage: www.elsevier.com/locate/ces

Design optimization of a 3-stage membrane cascade for oligosaccharides purification using mixed integer non-linear programming

Zulhaj Rizki [a,*], Anja E.M. Janssen [a], Eligius M.T. Hendrix [b], Albert van der Padt [a,c], Remko M. Boom [a], G.D.H Claassen [d]

[a] Wageningen University, Food Process Engineering Group, PO Box 17, 6700 AA Wageningen, the Netherlands
[b] Universidad de Málaga, Computer Architecture, Málaga, Spain
[c] FrieslandCampina, Stationsplein 4, Amersfoort 3818 LE, the Netherlands
[d] Wageningen University, Operational Research and Logistic Group, PO Box 8130, 6700 EW Wageningen, the Netherlands

HIGHLIGHTS

- MINLP is used to optimize a 3-stage nanofiltration cascade for FOS purification.
- The model selects the optimum membrane, TMP, temperature and area in each stage.
- The solutions are used to map the optimum operating conditions in the cascade.
- In a 3-stage cascade, the top stage works as the critical separation stage.

GRAPHICAL ABSTRACT

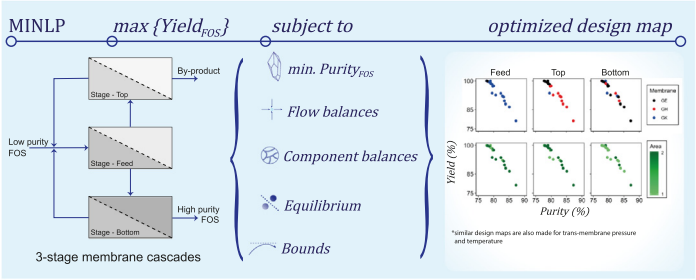

ARTICLE INFO

Article history:
Received 31 July 2020
Received in revised form 22 October 2020
Accepted 2 November 2020
Available online xxxx

Keywords:
Optimization
Membrane cascade
Process design
MINLP

ABSTRACT

Inhomogeneous membrane cascade systems have been utilized to purify fructooligosaccharides (FOS). Such a process allows a different setup at every stage of the cascade. Varying the setup at every stage implies an optimization problem related to the selection of the membrane and combinations of operating conditions. This paper solves the optimization problem for an inhomogeneous 3-stage membrane cascade and uses the solution as a design guideline. The optimization problem in the 3-stage membrane cascade design has been formulated as a mixed integer, non-linear programming model and solved using the global optimization solver, BARON. By maximizing the yield repetitively with varying purity requirements, a frontier curve has been constructed. The frontier curve was mapped showing the window of operation. The map guides towards the setup that promotes higher permeation in the feed stage when we switch from high yield to high purity. On the other hand, the setup selection at the bottom stage does not show a clear switch, which indicates that the selection at this stage is less critical.

1. Introduction

This paper contributes to the study of membrane separation processes for purification of fructooligosaccharides (FOS). A cascaded membrane system performs better than a single-stage separation (Caus et al., 2009; Lightfoot et al., 2008; Patil et al., 2014). A single membrane is limited by its inherent permeation and separation principles. This limit can be exceeded by creating more selective membranes, either using new materials or by modifying its surface (Lalia et al., 2013; Mohammad et al., 2015; Upadhyaya et al., 2018); but it is obvious that this approach has its limits. Besides changing the membrane, the separation can be improved by adding extra loops using available membranes, which

* Corresponding author.
E-mail address: zulhaj.zulhajrizki@wur.nl (Z. Rizki).

https://doi.org/10.1016/j.ces.2020.116275
0009-2509/

Nomenclature

Symbols

c	solute concentration (g/L)
Fl	flow rate (kg/h)
Sv	sieving coefficient (dimensionless)
y	binary variable selecting design option (dimensionless)

Subscripts

F	feed
P	permeate
R	retentate

Indices

a	membrane area
i	component, degree of polymerization
m	membrane type
p	*trans*-membrane pressure
s	stage in the cascade
t	operating temperature

is commonly known as a multi-stage membrane system (Siew et al., 2013). However, simply using membranes in series is inefficient. A configuration of membranes in series only processes 1 outlet stream (either the permeate or retentate) from the previous stage while losing the other stream. Valuable components may still be present in the lost stream causing a low yield. Recycling the streams in a cascaded configuration bypasses this issue, thus improving the product yield while allowing higher purity (Lightfoot et al., 2008; Patil et al., 2014).

The concept for an ideal 3-stage membrane cascade design was inspired by the design of a distillation column, and proposed by Lightfoot et al. (Lightfoot et al., 2008). In this design, both permeate and retentate from the first stage are fed to two additional membrane stages, giving a more refined permeate and a more concentrated retentate. The streams that are not taken as products are recycled and mixed with the feed stream (Fig. 1). According to the concept of the ideal cascade, these recycle streams should have a similar composition. This is the case only when both the separation factors and the size of the fluxes in all stages are exactly the same. This condition is hardly tenable in practice. Having dissimilar compositions of recycle streams implies that the cascade can be improved by allowing heterogeneous operating conditions and membranes among the stages. This design is known as an inhomogeneous cascade, which can give a better performance than an ideal cascade (Patil et al., 2014; Patil et al., 2015). Moreover, modification of the configurations of the cascade may increase the separation performance (Patil et al., 2016; Rizki et al., 2020).

However, the design of an inhomogeneous cascade is complicated. Varying the configuration of every stage, plus the operating conditions (e.g. *trans*-membrane pressure [TMP] and temperature) for every stage implies a challenge in the optimization of the design. The use of multiple stages gives a combinatorial increase in the number of possible configurations, and selecting one particular optimal combination is not trivial. A straightforward approach would be to enumerate and simulate all possible combinations and select the best outcomes. However, this requires unrealistically large computing power, given the number of possible configurations. To alleviate this, a subset of all possible combinations can be chosen (Rizki et al., 2020; Rizki et al., 2019) as representative, and a selection can be made within this subset. However, there is no guarantee that the globally best outcome is part of this subset.

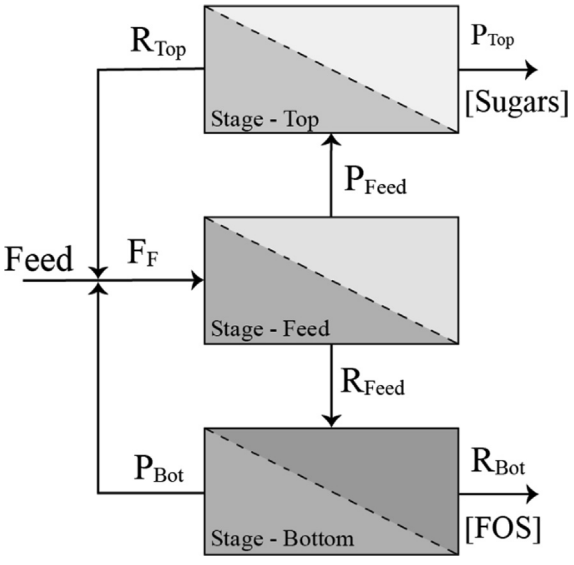

Fig. 1. Graphical representation of a 3-stage membrane cascade.

Another approach is to develop an optimization model and determine the best combination automatically. An optimization algorithm can be used to solve the model and ensure that the solution is optimal (Yang et al., 2013; Lin et al., 2012). This saves a lot of computation time because it avoids unnecessary evaluation of combinations that are far from optimal (Kronqvist et al., 2019; Anand et al., 2017; Boukouvala et al., 2016; Misener and Floudas, 2014; Ryoo and Sahinidis, 1995).

Here, we formulate the design of a 3-stage membrane cascade as a combinatorial, mixed integer, non-linear problem (MINLP). The membrane cascade is modelled to purify fructooligosaccharides (FOS) from mono- and disaccharides. FOS are commonly used as a prebiotic and rheology improver in many food products. However, their functionality is hindered due to the presence of small sugars; these add sweetness and caloric value to the oligosaccharides and are not prebiotic (Franck A.*, ; Meyer et al., 2011; Flamm et al., 2001; Tárrega et al., 2011; Hess et al., 2011). Purification of FOS using membrane processes has been done previously (Goulas et al., 2002; Kuhn et al., 2010; Machado et al., 2016), and earlier studies showed that a modified, inhomogeneous cascade can perform better than homogeneous, ideal cascades in terms of product purity and yield (Rizki et al., 2019; Aguirre Montesdeoca et al., 2016), even though these systems were not yet fully optimized.

In previous work, membrane cascades were optimized by scenario simulations of a limited set of configurations and choosing the best performing setup (Rizki et al., 2019). This method is not effective, because there is no guarantee that these selected systems are optimal. An alternative route is to optimize the membrane cascade design and the process parameters at the same time using MINLP, which, to the best of our knowledge, is a new approach in designing inhomogeneous membrane cascades. Applications of MINLP to optimize cascaded membrane systems can be found in several publications (Adi et al., 2016; Khor et al., 2011; Aliaga-Vicente et al., 2017). However, these applications only considered ideal cascades and focused the optimization on the superstructure of the cascades. Optimization of an inhomogeneous cascade with respect to the combination of its operating conditions, as presented in previous research (Rizki et al., 2020; Rizki et al., 2019; Rizki et al., 2020), has not been studied yet. This numerical approach to optimize a 3-stage membrane cascade for FOS purification using an MINLP is presented in this paper.

2. Model formulation

A 3-stage cascade model is developed based on the performance of a single-stage model. Each stage in the cascade can be operated using a different type of membrane and a different TMP, temperature and membrane area. These variables are the independent design variables that describe the selection of options at each stage. The performance of a single-stage membrane is characterized by the permeate flow rate, Fl_P, and the observed sieving coefficient, Sv. These values determine the feed conditions of the consecutive stages and consequently the outlet streams. Numerical optimization can be performed to select the best setup with respect to the outlet stream.

2.1. Input data and variable declaration

The permeate flow rate, Fl_P, and the observed sieving coefficient, Sv, depend on the independent operating variables, as is specified in Table 1. In this table, the argument m represents the membrane type that can be used in stage s (1, 2 or 3). The arguments p and t represent the TMP and the temperature applied, and the argument a refers to the membrane area. Because in practice membranes are supplied as modules with a specific membrane surface area, the value of a can be represented by the number of identical membrane modules used in parallel, and thus in our approach, it is a discrete value. The sieving coefficient is not dependent on the surface area of the membrane and is the same for every identical module that is used in parallel. However, the value of the sieving coefficient varies for every component, i. In a mixture of FOS, the component i represents carbohydrates with a varying degree of polymerization (DP).

The values of Fl_P and Sv for a given configuration m, p, t, a and i can be obtained either via experiments or via a model. The effects of the operating variables on the flow rate and sieving coefficient are neither straightforward nor linear. A recent publication explains the mechanistic relation between the input variables and the flow rate and sieving coefficient (Rizki et al., 2020). Direct incorporation of this mechanism into an optimization model is possible but will result in a complex optimization model, which may cause the model to become computationally intensive and may even become unsolvable. Alternatively, we can evaluate the mechanistic model under a wide range of conditions and apply the result as an input dataset for the optimization model. This will strongly decrease the computational effort during the optimization, while still capturing the response of the full model.

The value of the permeate flow rate does not depend on the stage. However, the retentate flow rate does. The permeate flow rate values are included in the input dataset while the retentate flow is related to the permeate flow via a mass balance (Eq. 1), which also depends on the feed flow. The flow enters each stage in a different condition, and therefore the retentate flow also depends on the stage position (Eq. 3).

$$Fl_{F,s} = Fl_{P,s} + Fl_{R,s} \quad \text{for all stages } s \tag{1}$$

$$c_{F,s,i}Fl_{F,s} = c_{P,s,i}Fl_{P,s} + c_{R,s,i}Fl_{r,s} \quad \text{for all stages } s \text{ and components } i \tag{2}$$

These mass balances in every stage also relate the concentration of every flow that comes in and out of the stage (Eq. 2). The concentration in the permeate and retentate flows of a stage are related through the observed sieving coefficient (Eq. 3). This observed sieving coefficient, Sv, varies as a function of the membrane type, the TMP and the temperature.

$$Sv_i = \frac{c_{P,i}}{c_{R,i}} \quad \text{for all components } i \tag{3}$$

Incorporating the stage indication s, as an argument together with the operating variables (m, p, t and a) creates a combinatorial option at each stage.

To select the optimal combination of m, p, t, a, the binary variable $y(s, m, p, t, a)$ is introduced for each stage s. The task is to find the best combination of m, p, t, a at each stage. Therefore, the variable y should be binary ($y \in \{0, 1\}$); it is or it is not the optimal combination. Because only one single combination of m, p, t, a exists at every stage s, the sum of $y(s, m, p, t, a)$ should be 1 for each stage. This variable permits generalizing the model and optimizing the design effectively: Multiplying $y(s, m, p, t, a)$ with all options will negate all non-optimal combinations and only give 1 optimal combination for each stage.

The system is assumed to be in a steady state. In the 3-stage cascade configuration, the permeate from the feed stage, P_F, becomes the feed stream for the top stage, F_{Top}. The retentate, R_{Feed}, becomes the feed for the bottom stage, F_{Bot}. The retentate from the top stage and the permeate from the bottom are recycled and mixed with the original feed stream. The mixed stream is then fed to the feed stage. The flow rate and concentrations of that mixed feed stream can also be calculated via mass balances (Eqs. 4 and 5).

$$Fl_{FF} = Fl_{Feed} + Fl_{R,Top} + Fl_{P,Bot} \tag{4}$$

$$c_{FF,i}Fl_{F_F} = c_{Feed,i}Fl_{Feed} + c_{R,Top,i}Fl_{R,Top} + c_{P,Bot,i}Fl_{P_{Bot}} \quad \text{for all components } i \tag{5}$$

Solving the mass balances in the mixing point is not straightforward. We can only calculate the recycle streams after knowing the outlet from the feed stage. However, solving the mass balance in the feed stage requires the condition of its feed, which is the unknown mixed stream. This is not an issue in the ideal cascade concept, because it assumes identical concentrations from the streams entering the mixing point. The previous model for membrane cascades (Rizki et al., 2020; Rizki et al., 2019) solved this problem iteratively; estimating the mixed stream and repeating the calculation until the mass balance in Eq. (4) is met. However, in a constrained optimization model, this so-called pooling problem is known to be a rather challenging problem, and strategies have been developed to include this pooling problem in optimization procedures (Song and Elimelech, 1995; Wiebe et al., 2019). This turns the system into an MINLP. MINLP problems are often non-convex, in which local optima can be found rather than the global optimum. Therefore, solving such problems requires a global optimization solver.

Table 1
Process parameters and variables used in the optimization model.

Variables	Symbols	
Permeate flow rate with given design options(m, p, t, a)	$Fl_P = f(m, p, t, a)$	(24)
Sieving coefficient of component i with given design (m, p, t)	$Sv = f(m, p, t, i)$	(25)
Retentate flow rate at stage s with given design options(m, p, t, a)	$Fl_R = f(s, m, p, t, a)$	(26)
Concentration of permeate stream at stage s for component$i$	$c_P = f(s, m, p, t, a, i)$	(27)
Concentration of retentate stream at stage s for component$i$	$c_R = f(s, m, p, t, a, i)$	(28)
Binary variable selecting design options for stages	$y = f(s, m, p, t, a)$	(29)

2.2. Purity and yield

The performance of a separation process is commonly assessed with the purity and yield of the product coming out of the system. The purity of a product is defined as a fraction of the main component in the product, in the total amount of solutes. In a mixture of FOS, oligosaccharides with DP3 or higher are considered to be the main product and the small sugars with DP2 and lower are contaminants to be removed. Therefore, we can formulate the purity and yield of FOS product coming from a 3-stage cascade as described in Eqs. (6) and (7).

$$\text{Purity} = \frac{\sum_{(i\geq 3)} c_{r,Bot}(i)}{\sum_i c_{r,Bot}(i)} \times 100\% \tag{6}$$

$$\text{Yield} = \frac{\sum_i c_{r,Bot}(i \geq 3) Fl_{r,B}}{\sum_i c_F(i) Fl_F} \times 100\% \tag{7}$$

2.3. Optimization problem

An optimization model is formulated to find the combination of membrane, TMP, temperature and membrane surface area for every stage of a 3-stage cascade that gives the best performance. For this, we formulate a maximization problem. The performance indicator can be represented by either the purity or the yield. By definition, using purity as the objective function may lead to a fractional objective (Yemets et al., 2006) because both the nominator and the denominator in Eq. (6) follow from the calculations. This is not the case with the yield as an objective. Therefore, the yield is a more appropriate objective. The purity is included as one of the constraints (Eqs. 8 and 9). A frontier curve can then be used to find optimal combinations for purity and yield.

The optimal configuration can be found by maximizing the yield subject to the set of constraints as described in Eqs. (9)–(23). The mass balances defined in the previous section are reformulated as constraints in Eqs. (11)–(19). In addition, some ranges are added as both lower and upper bounds for variables to limit the search area. The lower bounds need to be defined considering the computing sensitivity, whereas the upper bounds can be chosen arbitrarily according to experimental observation or data from the literature.

$$\max \text{ Yield} \tag{8}$$

subject to

(Minimum requirements)

$$\text{Purity} \geq Low_{\text{Purity}} \tag{9}$$

$$\sum_{m,p,t,a} y(s,m,p,t,a) = 1 \text{ for all } s \in \{\text{top}, \text{feed}, \text{bottom}\} \tag{10}$$

(Flow balances)

$$Fl_{FF} = Fl_F + \sum_{m,p,t,a} \left[Fl_r(\text{Top},m,p,t,a) + y(\text{Bottom},m,p,t,a) \cdot Fl_p(m,p,t,a)\right] \tag{11}$$

$$Fl_{FF} = \sum_{m,p,t,a} \left[y(\text{Feed},m,p,t,a) \cdot Fl_p(m,p,t,a) + Fl_r(\text{Feed},m,p,t,a)\right] \tag{12}$$

$$\sum_{m,p,t,a} \left[y(\text{Feed},m,p,t,a) \cdot Fl_p(m,p,t,a)\right] = \sum_{m,p,t,a} \left[y(\text{Top},m,p,t,a) \cdot Fl_p(m,p,t,a) + Fl_r(\text{Top},m,p,t,a)\right] \tag{13}$$

$$\sum_{m,p,t,a} Fl_r(\text{Feed},m,p,t,a) = \sum_{m,p,t,a} \left[y(\text{Bottom},m,p,t,a) \cdot Fl_p(m,p,t,a) + Fl_r(\text{Bottom},m,p,t,a)\right] \tag{14}$$

(Concentration equilibrium)

$$Sv(m,p,t,i) \cdot \sum_a c_r(s,m,p,t,a,i) = \sum_a c_p(s,m,p,t,a,i) \text{ for all } s,m,p,t \text{ and i} \tag{15}$$

(Component balances)

$$c_{FF}(i) \cdot Fl_{FF} = c_F(i) \cdot Fl_F + \sum_{m,p,t,a} \left[c_p(\text{Bottom},m,p,t,a,i) \cdot y(\text{Bottom},m,p,t,a) \cdot Fl_p(m,p,t,a) + c_r(\text{Top},m,p,t,a,i) \cdot Fl_r(\text{Top},m,p,t,a)\right] \text{ for all components} \tag{16}$$

$$c_{FF}(i) \cdot Fl_{FF} = \sum_{m,p,t,a} \left[c_p(\text{Feed},m,p,t,a,i) \cdot y(\text{Feed},m,p,t,a) \cdot Fl_p(m,p,t,a) + c_r(\text{Feed},m,p,t,a,i) \cdot Fl_r(\text{Feed},m,p,t,a)\right] \tag{17}$$

$$\sum_{m,p,t,a} \left[c_p(\text{Feed},m,p,t,a,i) \cdot y(\text{Feed},m,p,t,a) \cdot Fl_p(m,p,t,a)\right] = \sum_{m,p,t,a} \left[c_p(\text{Top},m,p,t,a,i) \cdot y(\text{Top},m,p,t,a) \cdot Fl_p(m,p,t,a) + c_r(\text{Top},m,p,t,a,i) \cdot Fl_r(\text{Top},m,p,t,a)\right] \tag{18}$$

$$\sum_{m,p,t,a} \left[c_r(\text{Feed},m,p,t,a,i) \cdot Fl_r(\text{Feed},m,p,t,a)\right] = \sum_{m,p,t,a} \left[c_p(\text{Bottom},m,p,t,a,i) \cdot y(\text{Bottom},m,p,t,a) \cdot Fl_p(m,p,t,a) + c_r(\text{Bottom},m,p,t,a,i) \cdot Fl_r(\text{Bottom},m,p,t,a)\right] \tag{19}$$

(Bounds)

$$\text{Low}_{Fl} \leq Fl_r \leq \text{Up}_{Fl} \text{ for all } s,m,p,t,a \tag{20}$$

$$Fl_r \geq \text{Low}_{rat} \cdot y \cdot Fl_p \text{ for all } s,m,p,t,a \tag{21}$$

$$c_r(s,m,p,t,a,i) \leq \text{Up}_c \text{ for all } s,m,p,t,a,i \tag{22}$$

$$c_p(s,m,p,t,a,i) \leq \text{Up}_c \text{ for all } s,m,p,t,a,i \tag{23}$$

The solution of Eqs. (8) to (23) is a set of binary variables, $y(s,m,p,t,a) \in \{0,1\}$ for each stage and for all possible combinations of membrane types, TMPs and areas. Among those combinations, there are only 3 variables y with values of 1 corresponding to the 3 stages of the cascade. These $y$values describe the optimal combination for every stage.

3. Methods

3.1. Feed condition

The optimization model is in line with a model that was used in previous study (Rizki et al., 2020), in which a mixture of FOS was fed into a 3-stage membrane cascade system resulting in a higher purity of the product. This previous model simulated the outcome of both single- and 3-stage systems with a given membrane, TMP, temperature and membrane area at each stage. Here, that model is referred to as the *sim* model.

The current model was developed based on mathematical programming. This model is further referred as the MP model. Both the MP and the *sim* models use a pre-defined feed stream, which contains a mixture of oligosaccharides with a DP from 1 to 10. The oligosaccharides with DP higher than 5 are clustered as 1 com-

Table 2
Feed concentration for the optimization model.

Index value, i	Component	Concentration for characterization (g/L)[a]
1	DP1	0.380 ± 0.022
2	DP2	0.396 ± 0.024
3	DP3	0.706 ± 0.049
4	DP4	0.769 ± 0.050
5	DP $\geq$ 5	1.329 ± 0.089

[a] Uncertainties are calculated based on the 95% confidence interval for all experiments.

Table 3
Values of the operating design variables used in the optimization model.

Decision variables	Indices	Levels
Stage	s	Feed, top, bottom
Membrane	m	GE, GH, GK
TMP	p	4, 8, 10, 12, 14, 16bar
Temperature	t	25 °C, 30 °C, 35 °C, 40 °C, 45℃
Area	a	1and2

ponent, so we have 5 components in the system. The component composition of this feed stream is summarized in Table 2. The feed enters the system at a flow rate of 60 kg/h.

3.2. Design variables

The search for the optimum configuration was done with 5 independent operating variables to be optimized: for each stage, s, we chose a membrane type, m, TMP, p, temperature, t, and membrane area, a (Table 3). For each of the 3 stages in the cascade design, the binary variable y represents the choices of the design variables. The constraints (Eqs. (9)–(23)) ensured that only 1 combination of the design variables would be selected for every stage.

The membrane variable represents the available choice of membranes. Three different membranes from General Electric were used: GE with molecular weight cutoff (MWCO) of 1 kDa, GH with MWCO of 2.5 kDa and GK with MWCO of 3.5 kDa. These 3 membranes were used with a TMP of 4–16 bar and at a temperature of 25 °C–45℃. These variables are continuous and may take any value within the indicated ranges. However, a continuous variable in the model requires a defined relationship between the independent variables and the dependent variables. These relations between TMP, temperature and membrane properties exist but are complex. Therefore, for the optimization model, we simplified the problem by only using a discrete set of values for these variables.

In practice, membranes are offered in modules with a specific membrane surface, therefore we also assume that the membrane surface area can only be a multiple of the surface of identical modules. We considered using 1 or 2 modules per stage in the MP mode with a surface area of 0.38 m^2 per module. Because the surface area per module was fixed, we only show the number of modules as the input variable. The relationship between the surface area and the permeate flow rate is linear and does not affect the sieving coefficient.

3.3. Dataset of single-stage membranes

The performance of a single stage is represented by its permeate flow rate and its sieving coefficient. Both flow rate and sieving coefficient depend on the independent operating parameters (Table 3). The performance of a single membrane is assumed to be consistent and thus independent of the stage position. The sieving coefficient does not depend on the membrane area, but the permeate flow rate scales linearly with the surface area. Apart from this, the permeate flow rate depends on the type of membrane, the TMP and the temperature. Both sieving coefficient and the permeate flow rate can be simulated using a modified steric-pore model with known characteristics of the membranes (pore size and hydrodynamic resistance) under specific TMP and temperature (Rizki et al., 2020). With this model, the permeate flows and sieving coefficient were simulated with a complete factorial combination of m, p and t at all levels (Table 3). This lookup table for single-stage separations (see Supplementary Table S.1) was then used in the optimization procedure.

3.4. Optimization model and validation

The optimization problem was written using the general algebraic modelling system (GAMS). This system allows different solvers related to many optimization problems to be used. We used the network-enabled optimization system (NEOS) (Czyzyk et al., 1998) using a global optimization solver, BARON. This solver follows a branch-and-bound algorithm to ensure that the found optimum is global (Kılınç and Sahinidis, 2018; Sahinidis, 1996; Sahinidis, 2003).

Before the optimization, the MP model was validated using the *sim* model in predicting both the purity and yield of a 3-stage FOS fractionation. The *sim* model itself was previously validated using experimental data under various conditions (Rizki et al., 2020). Using the *sim* model to validate the new MP model allowed us to test any combination, which might have not been possible experimentally.

Combinations of the operating variables were used as input variables. For validation purposes, we used a fractional factorial design to generate combinations of input variables. This design considered all 3 types of membranes, 3 levels of TMPs (8, 12 and 16 bar), 3 levels of temperatures (25 °C, 35 °C and 45℃) and 2 level of membrane area for every stage. There were 324 possible combinations of these input variables. The generation of these combinations was done using a fractional factorial design table from the literature (Chen et al., 1993). Not all combinations were feasible due to insufficient flow. Excluding the infeasible combinations, 132 combinations remained to be validated.

4. Results and discussion

4.1. Model validation

The MP model was validated using the *sim* model with 132 independent combinations of values for the process variables (Fig. 2). The horizontal axis represents all 132 combinations that were considered for validation. These combinations are sorted based on the predicted yield value. We hardly see any differences between the model outcomes, at higher yields. However, differences become larger at smaller yields.

The deviations between the MP and *sim* model stem from the inability of the MP model in handling continuous concentration variations in streams. The MP model uses fixed values of the permeate flow rate and observed rejection with a given membrane type, TMP and temperature, whereas the *sim* model calculates the exact values. Differences in concentration will change the concentration polarization, which affects the permeate flux, because the osmotic pressure over the membrane changes. Fig. 3a shows that there are differences in the flux predicted by the *sim* model and that predicted by the MP model. However, as concentration polarization in nanofiltration remains relatively insignificant, the effect on the sieving coefficient remains small (Fig. 3b).

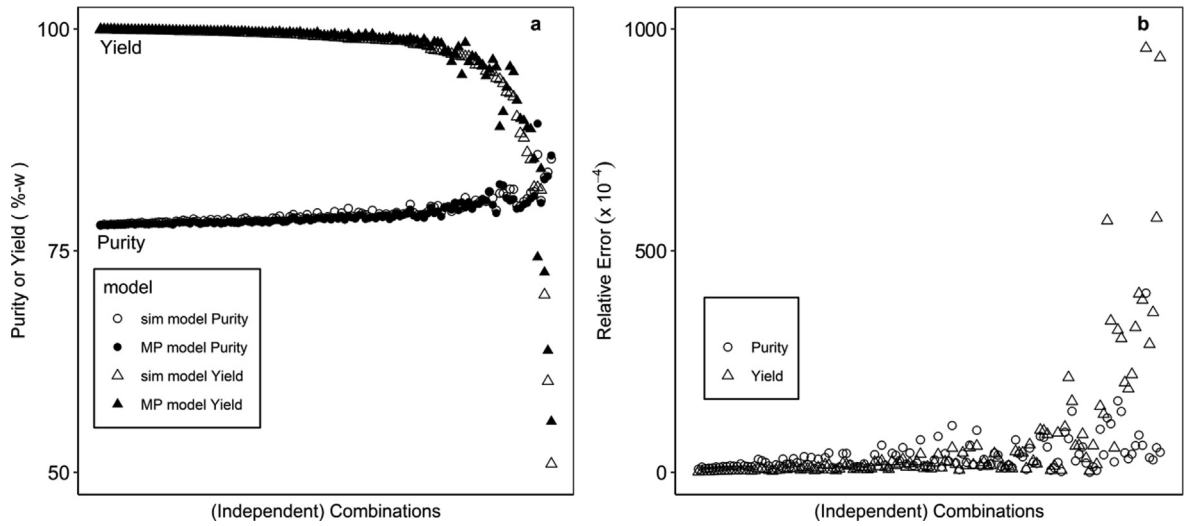

Fig. 2. Validation of the MP model using the *sim* model in predicting purity and yield with various combinations of setup shown as (a) the absolute values and (b) relative difference from the simulation model The Relative Error is defined as the difference of the values in figure (a) for both models divided by the value of simulation model.

Despite the differences, the MP model gives predictions of the purity and yield that agree well with the *sim* model. A paired *t*-test analysis for both models shows that there is no significant difference between these 2 models in predicting the purity and yield (within a 95% confidence interval). The differences are just 0.18% in the purity and 0.29% in the yield (Table 4).

We therefore conclude that the MP model describes the purity and yield of a 3-stage cascade system with sufficient accuracy.

4.2. Model solution

Solving Eqs. (8)–(24) identifies a set of input variables (Table 1) that give the maximum yield subject to given constraints, such as the minimum purity. The binary variable y identifies the system layout that gives the maximum yield. There are exactly 3 y variables that have a value of 1, corresponding to each stage. Because this variable is a function of the operating variables, we can find which combination of operating variables is the best. As an example, Table 5 shows the combination of membrane type, TMPs, temperature and area that leads to the maximum yield given a minimum purity of 80%.

This solution gives an indication that the search for an optimum combination can be successfully done numerically. Considering all levels of the decision variables, a manual search means a search of millions of possible options, which is costly and impractical. Using the MP model, we can easily find other optimal combinations when we require different purities.

4.3. Trade-off of best case scenarios

We constructed a frontier curve by optimizing the system using various purity requirements. Due to the discretization, the model could not give solutions at every purity value. The model either gave a solution with a higher purity than required or the problem became non-convergent. This problem resulted in gaps between the solutions on the frontier curve. More solutions in these gaps

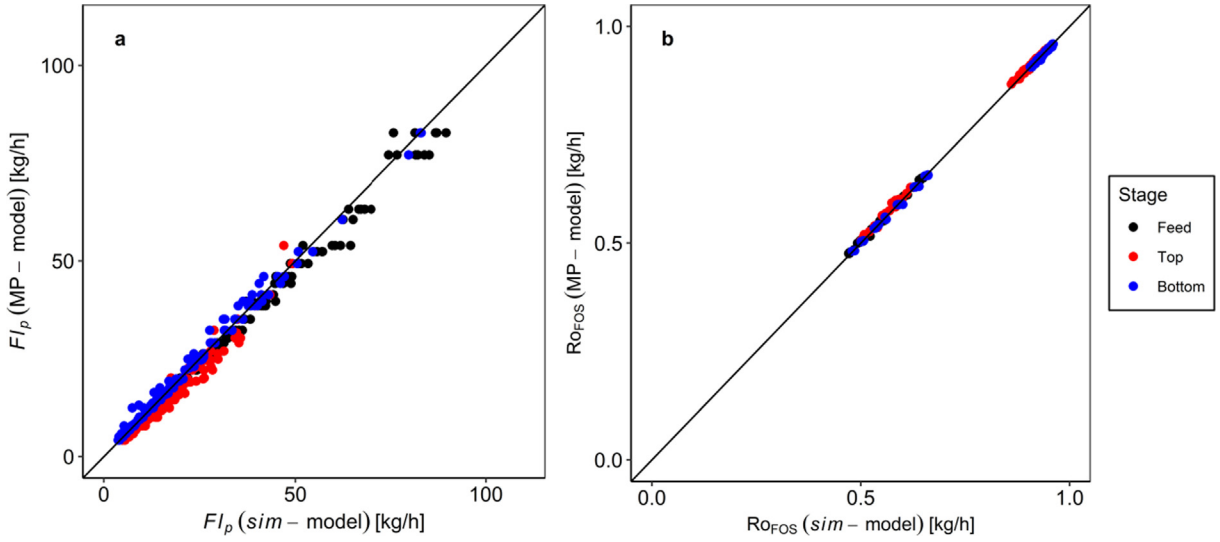

Fig. 3. Parity plot between the *sim* model and the MP model in predicting (a) the flow rate and (b) FOS observed sieving coefficient for each stage of the cascade system.

Table 4
Paired *t*-test result between the MP model and the *sim* model in predicting purity and yield.

Predictor	Difference between models (95% confidence interval)	*P* values
Purity (%)	0.11–0.26	2.19×10^{-6}
Yield (%)	0.51–0.73	0.009

Table 5
The solution for the optimization model with minimum purity 80%.

Parameters	Value
Minimum purity (%)	80
Purity (%) (constraint)	80.01
Yield (%) (optimization result)	97.43
Stage feed	
Membrane	GK
TMP (bar)	16
Temperature (℃)	45
Area	2
Stage top	
Membrane	GH
TMP (bar)	10
Temperature (℃)	30
Area	2
Stage bottom	
Membrane	GE
TMP (bar)	4
Temperature (℃)	35
Area	1

were found by using smaller steps in the required purity. As can be observed from Fig. 4, this resulted in smaller gaps (from black to red to blue symbols). A purity requirement lower than 77% is does not make sense, because the feed mixture itself has a purity of 77% and therefore all solutions already have a purity of more than 77%.

Like any other numerical method, the ability of the MP model to solve the optimization problem depends on the starting point. Using smaller step sizes decreases the distance of the starting point to the solution, and thus more solutions can be found. The step size, Δ, is defined as the increment of the minimum purity constraint while solving the optimization model repeatedly.

In the solver algorithm, a search is terminated when the difference between the latest solution and the previous iteration in the iteration is below a (pre-defined) threshold accuracy. The model may give different solutions depending on this threshold. This threshold should be defined relative to the size of the objective values. We observed that multiplying the purity and yield with certain numbers created different solutions (Table 6), because all these solutions are quite close to each other in terms of the objective value (here, the yield with the purity as constraint). The differences are often insignificant in practice. However, a small difference might come from totally different configurations. Table 6 illustrates this for model solutions with a maximum yield of 98% with purity of 79%. The combinations of purity and yield were chosen arbitrarily as an example. For the feed (middle) stage, all solutions use a GK membrane with some difference in pressures and temperatures. For the bottom stage, the solutions vary strongly. Our conclusion is that while the feed stage is critical, the bottom stage is not so critical for the optimization criterion, and therefore, freedom in the design is allowed here. Thus, we see that the optimization gives us an indication of the priorities in the design process and also provide alternative options for the other parts.

A finer resolution may help in finding solutions within the gaps between solutions found with a coarser resolution. This finer resolution was obtained by multiplying both yield and purity values

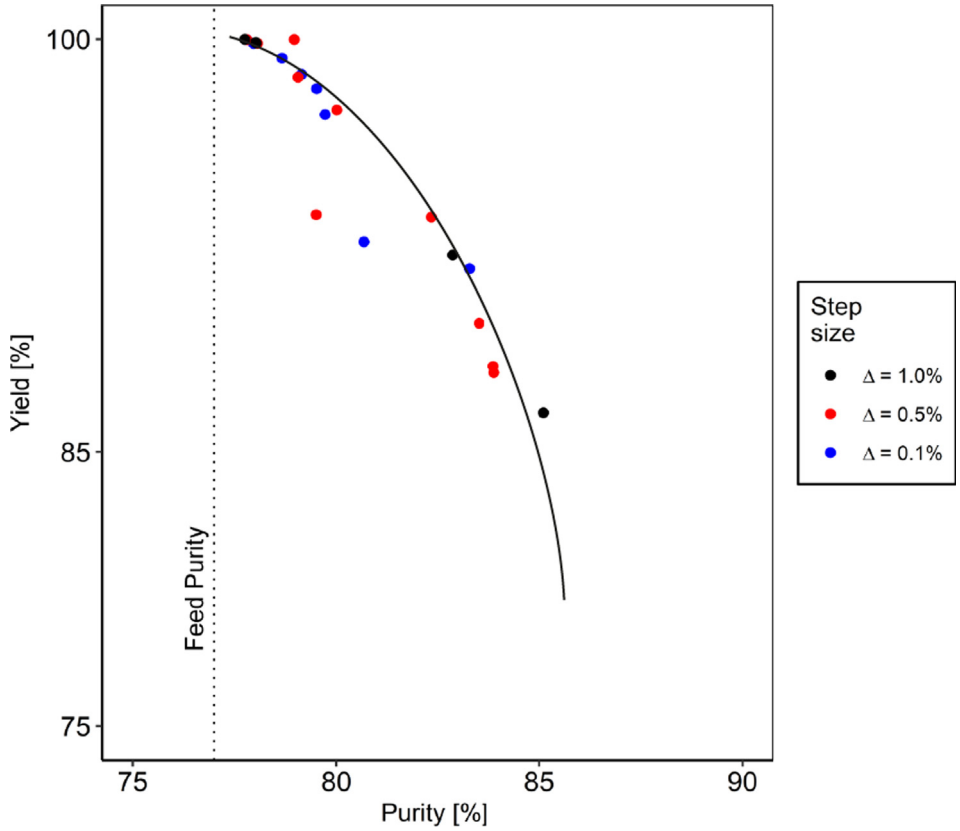

Fig. 4. Frontier curve and model solutions with different step size for setting the minimum purity.

Table 6
Solutions for the optimization model with purity 79% using different resolutions.

Parameters	Value (different resolutions)			
Resolutions	1×	10×	100×	1000×
Purity	79.06	79.52	79.13	79.39
Yield	98.62	98.23	98.39	98.00
Stage feed				
Membrane	GK	GK	GK	GK
Pressure	16	16	14	14
Temperature	40	45	35	35
Area	1	2	1	1
Stage top				
Membrane	GE	GH	GH	GH
Pressure	10	10	12	16
Temperature	40	25	35	25
Area	2	2	1	1
Stage bottom				
Membrane	GH	GE	GK	GE
Pressure	4	4	16	8
Temperature	35	30	40	25
Area	1	1	2	1

with arbitrary constants. By doing so, the model sensitivity was improved. However, the computational capacity restricts the resolution at some point. Fig. 5 shows that because of this, less solutions are found at 100 × and 1000 × resolutions. Thus. we conclude that there is an optimal resolution in term of the ability to find solutions. Among the resolution values presented in Fig. 5, resolution of 1000x is the best resolution in term of the coverage in the frontier curve. However, this resolution has fewer solution points, which is filled in by the other resolution values.

The MP model still gives some solutions below the frontier curve. These solutions are not real optima. However, somehow the solver recognized them as optimum solutions. Looking closer at those problems, these solutions have purities that are much higher than the requirement. Solving this issue can be done by finding a strategy to ensure that the purity constraint is binding. Another way is to add an extra constraint such as a minimum yield or maximum purity. However, the values of these constraints will necessarily be educated guesses, because we can only get good estimates after we have constructed the frontier. Moreover, the addition of an extra constraint increases the model complexity, which may lead to an unsolvable problem.

In Section 2.3. we discussed the difference in using the purity as a constraint and the yield as the optimization objective, and the use of the purity as the objective with the yield as constraint.

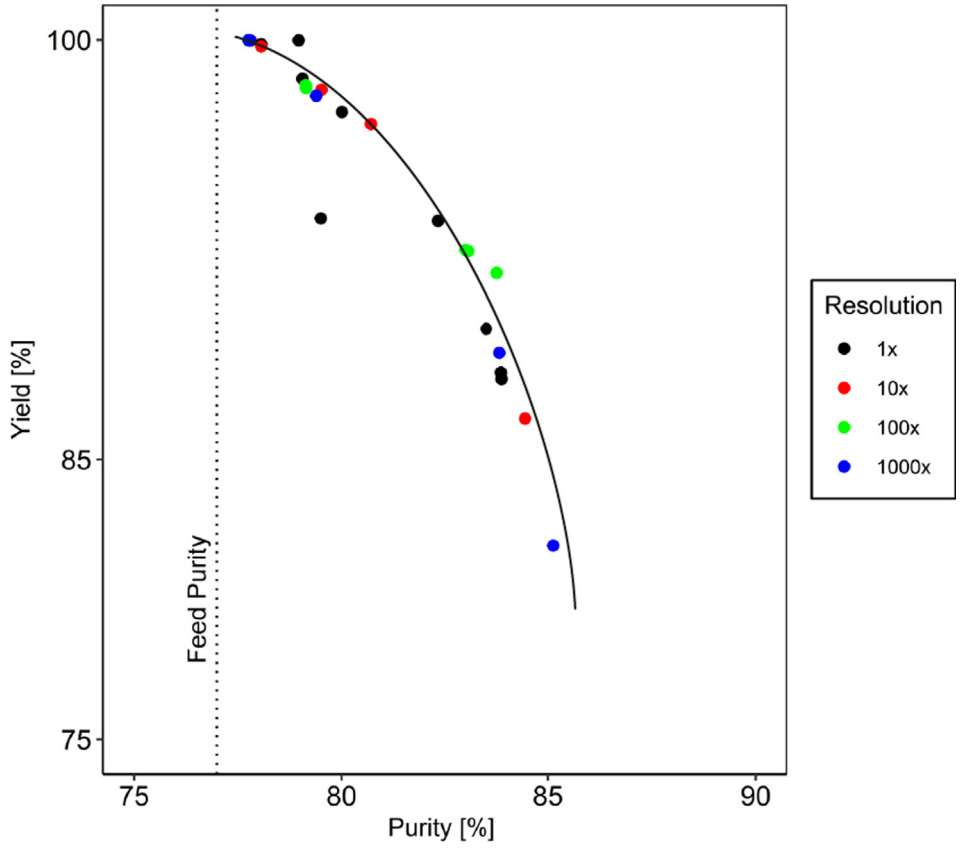

Fig. 5. Frontier curve and model solutions for various resolutions.

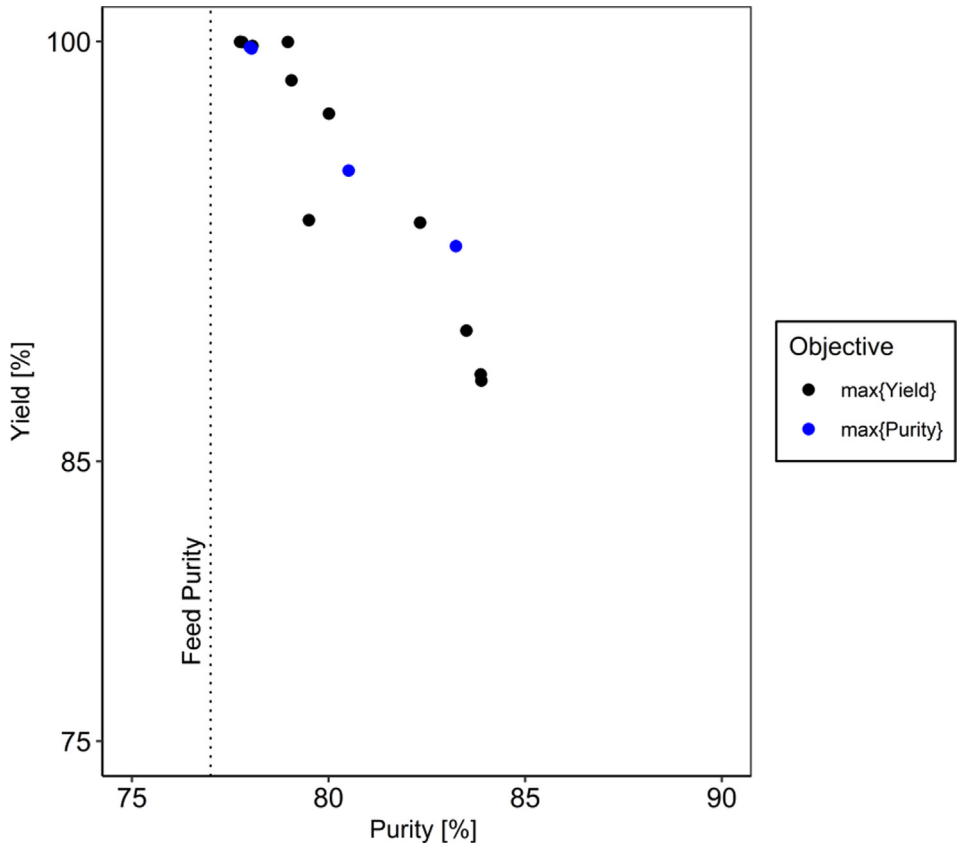

Fig. 6. Optimal solutions with different objectives: maximizing yield and maximizing purity simultaneously using the BARON solver.

Fig. 6 shows the results for both approaches. The solutions found by using the purity as the objective are in the same frontier curve found by using the yield as the objective. However, there is a numerical difference. The use of a global mixed integer quadratic programming solver (ANTIGONE) did not lead to a solution when maximizing purity, whereas BARON, which uses deterministic global optimization algorithms of the branch-and-bound type was able to attain solutions. It is therefore important to formulate the objective towards the specific algorithm that is chosen. This limitation can also be shown when less solution points are found while maximizing the purity.

It is also possible to optimize both criteria, purity and yield, simultaneously, by combining them in a single objective function. We expect that the solutions will follow the frontier line, with the precise location dictated by the weights that are assigned for the two factors.

4.4. Maps of best operating conditions

The frontier curve that is constructed is important because it gives the best possible performance by the system. In addition, analysing the configurations that give this best performance may offer guidelines on how to design cascaded membrane systems. Fig. 7 shows a map of the configurations and operating conditions along the frontier. This map gives a great contribution and insight in designing a membrane system, which conventionally done via *trial and error* or subjective guesses. With this map, a process designer can determine which operating condition to chose in each stage objectively.

A membrane with a low MWCO, the GE membrane, in the feed stage is only recommended when a very high yield is requested. The consequence of this is low purity; other components will also be partially retained. For higher purity at the expense of the yield, the membrane with the largest MWCO is chosen for the feed stage, the GK membrane. The intermediate membrane, the GH membrane, with MWCO in between the other membranes, is never optimal in the feed stage. The feed stage therefore mostly acts as a flow divider and not as the main purification stage.

For the top stage, a tight membrane (GE) is chosen for the highest yields, but for all other conditions, the intermediate membrane (GH) is chosen. The role of this stage in those latter cases is to polish the stream by removing some lower molecular weight components to obtain the required purity. Some loss of the high molecular wright components into the permeate is accepted, because this is returned to the feed stage, which will then redirect it again to the top stage. The membrane with the largest MWCO is never optimal for the top stage, because the permeate of the top stage is considered as waste.

In the bottom stage, we see more mixed configurations. All 3 membranes are selected at different sets of yield and purities. This implies that the choice of this membrane is not crucial, and the difference between different configurations is small. It may therefore be logical to choose the GK membrane, because this membrane is most open and will allow the largest flux, or the smallest membrane surface area.

Considering the operating conditions, we also see a clear trend. Higher pressure and temperature is optimal in the feed and top stages, whereas, on average, lower pressure and temperature is optimal in the bottom stage. However, also here, we see alternative selections of conditions for the bottom stage, indicating that the differences are not very large.

This supports previous studies in membrane cascading, which concluded that in the feed stage, a balanced flow is important, hence an open membrane can be used. Good separation is more

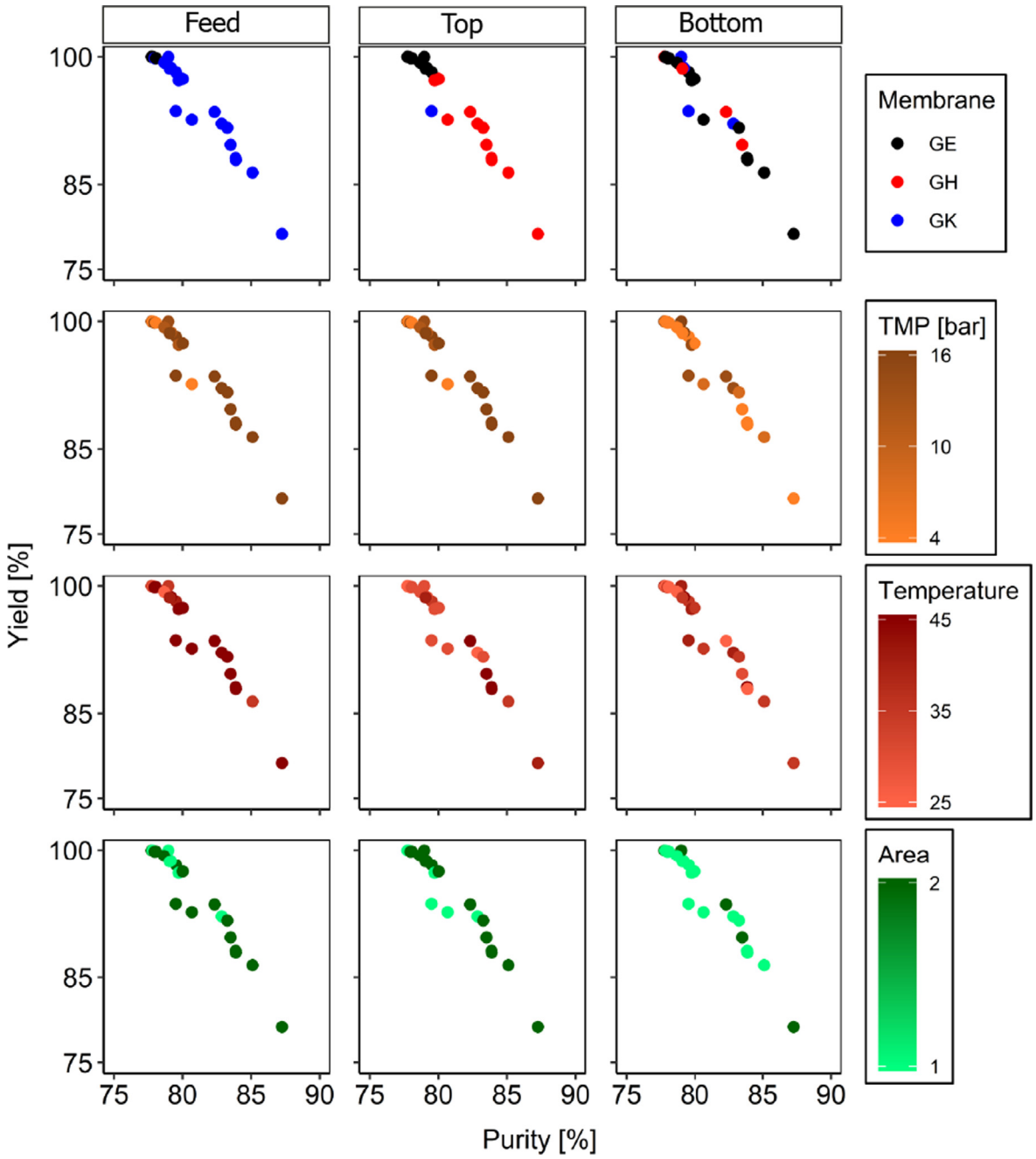

Fig. 7. Map of the operating conditions in the optimum solutions with yield higher than 75%.

crucial in the top stage; hence, a tighter membrane is chosen there, using a large TMP to ensure reasonable flux.

Unlike the feed and top stage, we cannot see a clear shift of the operating conditions in the bottom stage. We see that the choices are spread. This implies that the differences that are achieved by a specific choice in this stage do not greatly affect the yield and purity. We are therefore relatively free in the design for this stage; for example, based on other criteria, such as the required composition of the waste stream or on the minimization of the membrane surface area.

5. Conclusions

The design, configuration and choice of operating conditions in a 3-stage membrane cascade system for FOS purification were optimized numerically using a mixed integer non-linear programming. This mathematical programming model was validated using a previously validated simulation model under similar feed and operating conditions. This optimization problem was solved using the BARON algorithm to select a membrane, and the TMP, operating temperature and membrane surface area for each stage of the cascade to achieve the highest yield for a given required purity. The optimization can also be done by optimizing the product purity with a given yield requirement with comparable outcome.

We constructed a frontier curve from the optimized solutions that represents the optimum achievable combination of purity and yield with the cascade design. The frontier curve shows a trade-off between purity and yield in the process ranging from almost a complete recovery (99% yield) with low purity to maximum purity around 85% with a low yield. Mapping the configura-

tions and operating conditions on this frontier shows that to move from a high yield to a high purity, we need to increase the permeation in the feed stage by switching from a lower to a higher MWCO, and increase the TMP and temperature and membrane area. In the top stage, a membrane with a low MWCO is recommended, which minimizes the loss; for lower yields, a membrane with an intermediate MWCO is chosen. The design of the bottom stage is quite free and can be based on additional criteria, such as the composition of the waste product and minimization of the membrane surface area.

We can translate the finding into simple guidelines for designing inhomogeneous nanofiltration cascades:

1. The feed stage acts mainly as a flow divider; a membrane with relatively large MWCO should be chosen when high purity is preferred over a high yield; otherwise a membrane with a low MWCO should be chosen.
2. For the top stage, a membrane with a low MWCO is preferred when high purity is required; otherwise a membrane with an intermediate MWCO should be chosen.
3. The choice of the bottom stage membrane is not critical, and thus an open membrane with a larger flux may be chosen.

This study shows that optimization is useful to extract general design guidelines for complex process systems that go beyond idealized systems and can include non-ideal behaviour and experimental limitations (such as the size of modules that are available). Even with this, we can find design rules that can be applied in other designs without the need for a full optimization study.

Declaration of Competing Interest

The authors declare that they have no known competing financial interests or personal relationships that could have appeared to influence the work reported in this paper.

Acknowledgements

The authors would like to acknowledge Lembaga Pengelola Dana Pendidikan (LPDP), and Kementrian Keuangan Indonesia for financial support. The authors would also like to acknowledge the MSc students who have contributed to the model development: Marlijn Orbons, Afke Politiek and Rimke Braakman. Funding from the Spanish Ministry (RTI2018-095993-B-I00), in part financed by the European Regional Development Fund (ERDF) is also acknowledged.

Appendix A. Supplementary data

Supplementary data to this article can be found online at https://doi.org/10.1016/j.ces.2020.116275.

References

Caus, A., Braeken, L., Boussu, K., Van der Bruggen, B., 2009. The use of integrated countercurrent nanofiltration cascades for advanced separations. J. Chem. Technol. Biotechnol. 84 (3), 391–398.

Lightfoot, E.N., Root, T.W., O'Dell, J.L., 2008. Emergence of Ideal Membrane Cascades for Downstream Processing. Biotechnol. Prog. 24 (3), 599–605.

Patil, N.V., Janssen, A.E.M., Boom, R.M., 2014. The potential impact of membrane cascading on downstream processing of oligosaccharides. Chemical Engineering Science 106, 86–98.

Lalia, B.S., Kochkodan, V., Hashaikeh, R., Hilal, N., 2013. A review on membrane fabrication: Structure, properties and performance relationship. Desalination 326, 77–95.

Mohammad, A.W., Teow, Y.H., Ang, W.L., Chung, Y.T., Oatley-Radcliffe, D.L., Hilal, N., 2015. Nanofiltration membranes review: Recent advances and future prospects. Desalination 356, 226–254.

Upadhyaya, L., Qian, X., Ranil Wickramasinghe, S., 2018. Chemical modification of membrane surface — overview. Current Opinion in Chemical Engineering 20, 13–18.

Siew, W.E., Livingston, A.G., Ates, C., Merschaert, A., 2013. Continuous solute fractionation with membrane cascades – A high productivity alternative to diafiltration. Separation and Purification Technology 102, 1–14.

Patil, N.V., Janssen, A.E.M., Boom, R.M., 2014. Separation of Whey Proteins using Cascaded Ultrafiltration. Separation Science and Technology 49 (15), 2280–2288.

Patil, N.V., Feng, X., Sewalt, J.J.W., Boom, R.M., Janssen, A.E.M., 2015. Separation of an inulin mixture using cascaded nanofiltration. Separation and Purification Technology 146, 261–267.

Patil, N.V., Schotel, T., Rodríguez Gómez, C.V., Aguirre Montesdeoca, V., Sewalt, J.JW., Janssen, A.EM., Boom, R.M., 2016. Continuous purification of galacto-oligosaccharide mixtures by using cascaded membrane filtration: Membrane cascades for oligosaccharide purification. J. Chem. Technol. Biotechnol. 91 (5), 1478–1484.

Rizki, Z., Janssen, A.E.M., Claassen, G.D.H., Boom, R.M., van der Padt, A., 2020. Multi-criteria design of membrane cascades: Selection of configurations and process parameters. Separation and Purification Technology 237, 116349. https://doi.org/10.1016/j.seppur.2019.116349.

Rizki, Z., Janssen, A.E.M., Boom, R.M., van der Padt, A., 2019. Oligosaccharides fractionation cascades with 3 outlet streams. Separation and Purification Technology 221, 183–194.

Yang, X.-S., Koziel, S., Leifsson, L., 2013. Computational Optimization, Modelling and Simulation: Recent Trends and Challenges. Procedia Computer Science 18, 855–860.

Lin, M.-H., Tsai, J.-F., Yu, C.-S., 2012. A Review of Deterministic Optimization Methods in Engineering and Management. Mathematical Problems in Engineering 2012, 1–15.

Kronqvist, J., Bernal, D.E., Lundell, A., Grossmann, I.E., 2019. A review and comparison of solvers for convex MINLP. Optim Eng 20 (2), 397–455.

Anand, R., Aggarwal, D., Kumar, V., 2017. A comparative analysis of optimization solvers. Journal of Statistics and Management Systems 20 (4), 623–635.

Boukouvala, F., Misener, R., Floudas, C.A., 2016. Global optimization advances in Mixed-Integer Nonlinear Programming, MINLP, and Constrained Derivative-Free Optimization, CDFO. European Journal of Operational Research 252 (3), 701–727.

Misener, R., Floudas, C.A., 2014. A Framework for Globally Optimizing Mixed-Integer Signomial Programs. J Optim Theory Appl 161 (3), 905–932.

Ryoo, H.S., Sahinidis, N.V., 1995. Global optimization of nonconvex NLPs and MINLPs with applications in process design. Computers & Chemical Engineering 19 (5), 551–566.

Franck, A., 2002. Technological functionality of inulin and oligofructose. Br. J. Nutr. 87 Suppl 2, S287–S291. https://doi.org/10.1079/BJNBJN/2002550

Meyer, D., Bayarri, S., Tárrega, A., Costell, E., 2011. Inulin as texture modifier in dairy products. Food Hydrocolloids 25 (8), 1881–1890.

Flamm, G., Glinsmann, W., Kritchevsky, D., Prosky, L., Roberfroid, M., 2001. Inulin and Oligofructose as Dietary Fiber: A Review of the Evidence. Critical Reviews in Food Science and Nutrition 41 (5), 353–362.

Tárrega, A., Torres, J.D., Costell, E., 2011. Influence of the chain-length distribution of inulin on the rheology and microstructure of prebiotic dairy desserts. Journal of Food Engineering 104 (3), 356–363.

Hess, J.R., Birkett, A.M., Thomas, W., Slavin, J.L., 2011. Effects of short-chain fructooligosaccharides on satiety responses in healthy men and women. Appetite 56 (1), 128–134.

Goulas, A.K., Kapasakalidis, P.G., Sinclair, H.R., Rastall, R.A., Grandison, A.S., 2002. Purification of oligosaccharides by nanofiltration. Journal of Membrane Science 209 (1), 321–335.

Kuhn, R.C., Maugeri Filho, F., Silva, V., Palacio, L., Hernández, A., Prádanos, P., 2010. Mass transfer and transport during purification of fructooligosaccharides by nanofiltration. Journal of Membrane Science 365 (1-2), 356–365.

Machado, M.T.C., Trevisan, S., Pimentel-Souza, J.D.R., Pastore, G.M., Hubinger, M.D., 2016. Clarification and concentration of oligosaccharides from artichoke extract by a sequential process with microfiltration and nanofiltration membranes. Journal of Food Engineering 180, 120–128.

Aguirre Montesdeoca, V., Van der Padt, A., Boom, R.M., Janssen, A.E.M., 2016. Modelling of membrane cascades for the purification of oligosaccharides. Journal of Membrane Science 520, 712–722.

V.S.K. Adi, M. Cook, L.G. Peeva, A.G. Livingston, B. Chachuat, Optimization of OSN Membrane Cascades for Separating Organic Mixtures. In: Comput. Aided Chem. Eng., Elsevier B.V., 2016: pp. 379–384. https://doi.org/10.1016/B978-0-444-63428-3.50068-0.

Khor, C.S., Foo, D.C.Y., El-Halwagi, M.M., Tan, R.R., Shah, N., 2011. A Superstructure Optimization Approach for Membrane Separation-Based Water Regeneration Network Synthesis with Detailed Nonlinear Mechanistic Reverse Osmosis Model. Ind. Eng. Chem. Res. 50 (23), 13444–13456.

Aliaga-Vicente, A., Caballero, J.A., Fernández-Torres, M.J., 2017. Synthesis and optimization of membrane cascade for gas separation via mixed-integer nonlinear programming. AIChE J. 63 (6), 1989–2006.

Rizki, Z., Suryawirawan, E., Janssen, A.E.M., van der Padt, A., Boom, R.M., 2020. Modelling temperature effects in a membrane cascade system for oligosaccharides. Journal of Membrane Science 610, 118292. https://doi.org/10.1016/j.memsci.2020.118292.

Wiebe, J., Cecílio, I., Misener, R., 2019. Robust Optimization for the Pooling Problem. Ind. Eng. Chem. Res. 58 (28), 12712–12722.

Song, L., Elimelech, M., 1995. Theory of concentration polarization in crossflow filtration. Faraday Trans. 91 (19), 3389. https://doi.org/10.1039/ft9959103389.

Yemets, O.A., Barbolina, T.N., Chernenko, O.A., 2006. Solving optimization problems with linear-fractional objective functions and additional constraints on arrangements. Cybern Syst Anal 42 (5), 680–685.

Czyzyk, J., Mesnier, M.P., More, J.J., 1998. NEOS server. IEEE Comput. Sci. Eng. 5, 68–75. https://doi.org/10.1109/99.714603.

Kılınç, M.R., Sahinidis, N.V., 2018. Exploiting integrality in the global optimization of mixed-integer nonlinear programming problems with BARON. Optimization Methods and Software 33 (3), 540–562.

Sahinidis, N.V., 1996. BARON: A general purpose global optimization software package. J Glob Optim 8 (2), 201–205.

Sahinidis, N.V., 2003. Global optimization and constraint satisfaction: The branch-and-reduce approach. Lect. Notes Comput. Sci. (Including Subser. Lect. Notes Artif. Intell. Lect. Notes Bioinformatics) 2861, 1–16. https://doi.org/10.1007/978-3-540-39901-8_1.

Chen, J., Sun, D.X., Wu, C.F.J., 1993. A catalogue of Two-Level and Three-Level Fractional Factorial Designs with Small Runs. Int. Stat. Rev. 61, 131–145. https://doi.org/10.2307/1403599.